

1 Deactivation and Collective Phasic

2 Muscular Tuning for Pointing

3 Direction: Insights from Machine

4 Learning

5 **Florian Chambellant¹, Jeremie Gaveau¹, Charalambos Papaxanthis¹, Elizabeth**
6 **Thomas¹**

*For correspondence:

7 ¹Université Bourgogne Franche-Comté, INSERM CAPS UMR 1093, France

8

9 **Abstract** Arm movements in our daily lives have to be adjusted for several factors in response
10 to the demands of the environment, for example, speed, direction or distance. Previously, we
11 had shown that arm movement kinematics is optimally tuned to take advantage of gravity effects
12 and minimize muscle effort in various pointing directions and gravity contexts (*Gaveau et al.,*
13 *2016*). Here we build upon these results and focus on muscular adjustments. We used Machine
14 Learning to analyze the ensemble activities of multiple muscles recorded during pointing in
15 various directions. The advantage of such a technique would be the observation of patterns in
16 collective muscular activity that may not be noticed using univariate statistics. By providing an
17 index of multimuscle activity, the Machine Learning analysis brought to light several features of
18 tuning for pointing direction. In attempting to trace tuning curves, all comparisons were done
19 with respects to pointing in the horizontal, gravity free plane. We demonstrated that tuning for
20 direction does not take place in a uniform fashion but in a modular manner in which some
21 muscle groups play a primary role. The antigravity muscles were more finely tuned to pointing
22 direction than the gravity muscles. Of note, was their tuning during the first half of downward
23 pointing. As the antigravity muscles were deactivated during this phase, it supported the idea
24 that deactivation is not an on-off function but is tuned to pointing direction. Further support for
25 the tuning of the portions of the phasic EMG containing only negative activity was provided by
26 progressively improving classification accuracies with increasing angular distance from the
27 horizontal. Overall, these results show that the motor system tunes muscle commands to exploit
28 gravity effects and reduce muscular effort. It quantitatively demonstrates that phasic EMG
29 negativity is an essential feature of muscle control.

30

31 **Introduction**

32 How the brain plans and executes movements is a challenging question in the field of motor neuro-
33 science. The well-known 'problem of redundancy' (*Bernshtein, 1967; Latash, 2012*), implies that a
34 large number of joints and muscles must be coordinated to produce adaptive movements that ad-
35 vantageously interact with our environment (*Franklin and Wolpert, 2011; Farshchian et al., 2018*).
36 A fundamental aspect of this environment is the presence of gravity acceleration. Until now, the
37 neural control of movement has been mostly investigated using tasks where the mechanical ef-
38 fects of gravity were canceled (for example, moving in a constrained horizontal plane). However,
39 living organisms must continuously produce adaptable movements that interact with gravity. In

40 attempting to gain knowledge that can apply to real life situations, it is paramount to understand
41 gravity-related movement control. Previously, we demonstrated that the brain plans arm move-
42 ments whose kinematics are optimally tuned to take advantage of gravity effects and minimize
43 muscle effort (*Gaveau et al., 2016*). Across varied directions and gravity levels, ratios of accelera-
44 tion versus deceleration well supported our optimal integration of gravity hypothesis and falsified
45 the pre-existing hypothesis according to which the brain would use a tonic torque to compensate
46 for gravity effects (*Hollerbach and Flash, 1982; Atkeson and Hollerbach, 1985; Flanders and Her-
47 rmann, 1992*). However, as noticed by reviewers, an important caveat in our investigation and
48 claims was the lack of support from muscle activation patterns (see reviewers comments in the
49 Decision letter for *Gaveau et al. (2016)*). Since many different muscle contractions can give rise to
50 the same kinematics (*Burdet et al., 2001; Hagen and Valero-Cuevas, 2017*), whether muscle effort
51 truly incorporates the benefits to be obtained from gravity effects remained to be seen.

52 A qualitative demonstration of a muscular integration of gravity effects for effort minimization
53 was later provided in our study on monkeys and humans (*Gaveau et al., 2021*). Scrutinizing the
54 phasic activations of antigravity muscles i.e. the remaining activity after subtracting the part that
55 compensates for gravity torque (*Flanders and Herrmann, 1992; Flanders et al., 1996*) – we observed
56 that antigravity muscles systematically exhibited negative phases. These negative portions on pha-
57 sic muscle EMGs indicated that there was less activity in the muscle pattern than what is required
58 to compensate for gravity torque. Importantly, these negative phases happen when gravity is able
59 to help produce the arm motion i.e. during the acceleration of downward movements and during
60 the deceleration of upward movements (*Gaveau et al., 2021*). Analyzing the negativity of phasic
61 muscle activations has since helped to understand the effect of laterality on sensorimotor control
62 (*Poirier et al., 2022*) as well as its modification with increasing age (*Poirier et al., 2023*).

63 The above studies supporting the optimal integration of gravity hypothesis at the muscular
64 level remain rather coarse-grained. They investigated a limited number of muscles during purely
65 vertical and horizontal movements (*Gaveau et al., 2021; Poirier et al., 2022, 2023*). A better under-
66 standing of the integration of gravity in motor control requires a finer-grained investigation where
67 more directions and muscles are examined. In a previous study, we had reported on the kinemat-
68 ics of pointing movements performed in seventeen different directions (*Gaveau et al., 2016*). In
69 this same investigation, we had also recorded the activation patterns of nine muscles for eleven
70 participants but did not exploit the muscle activation results. The present study takes advantage
71 of this EMG dataset to provide a fine-grained analysis of phasic EMGs and examine how they may
72 incorporate the beneficial contribution of gravity for muscle effort minimization. An important
73 caveat in the existing literature is that no study has specifically quantified the importance of the
74 phasic EMG negativity in the overall muscle activation pattern. Whether this negativity represents
75 an important part of the neural signals producing body limb movements is still unknown. In addition,
76 recent reports in the domain of muscle synergies have emphasized the need to develop tools
77 that allow investigating such negative signals (*Scano et al., 2022; Brambilla and Scano, 2022; Scano
78 et al., 2023*).

79 As mentioned in the previous paragraph, the experiments for the study from *Gaveau et al.*
80 (*2016*) were accompanied by the simultaneous recording of muscular activity. As we had recorded
81 EMG activities from 9 muscles of 11 participants performing 12 pointings trials in 17 directions,
82 we ended up with 20196 EMG traces (recorded at 2000Hz). As in the case of many motor control
83 experiments, this constituted a big data base. Consequently, we employed a Machine Learning
84 (ML) technique to draw benefits from a multimuscle approach. By the latter, we refer to situations
85 in which patterns or clearer effects are seen with muscle groups rather than single muscles. The
86 specific approach used was one of binary classification in which EMG time series were automati-
87 cally classified as coming from a horizontal movement or from another angle. We have previously
88 used binary classification successfully to provide insight into Whole Body Pointing (*Tolambya et al.,
89 2011, 2012*) and gait (*Nair et al., 2010; Laroche et al., 2014*). Classification accuracy provides an in-
90 dicator of data separation. Poor separation in the EMGs would lead to poor classification accuracy



Figure 1. a) Illustration of the task (adapted from ©2016, Gaveau et al.). b) Shoulder muscles from which the EMGs are recorded.

91 while EMGs that are very different would lead to higher accuracy. The main Machine Learning clas-
92 sification technique used in the present study was Linear Discriminant Analysis. This algorithm
93 utilizes information on the mean and variance of each category to build a representation of the
94 group (Grimm and Yarnold, 2000; Johnson and Wichern, 2007; Izenman, 2008). One of the rea-
95 sons for choosing LDA is the greater ease for finding the factors which are critical in classification
96 success. This is in keeping with the spirit of explainable artificial intelligence (XAI) (Murdoch et al.,
97 2019; Arrieta et al., 2020). Algorithms like Support Vector Machines are more powerful classifiers
98 but harder to probe for the combination of features which are the most critical to classification
99 accuracy (Thomas et al., 2023). Nevertheless, as our previous studies have shown that they can
100 be successfully applied to the analysis of EMG data (Tolambya et al., 2011, 2012), we used the
101 technique as a supplementary method to reinforce the conclusions made using LDA.

102 **Method**

103 **Subject, task and recording**

104 The data used in the current investigation comes from a previous study by Gaveau et al. (2016). To
105 briefly summarize the task: 11 adults were asked to execute a pointing task. Participants started at
106 an initial position (shoulder elevation 90°, shoulder abduction 0°, arm completely stretched) then
107 proceeded to rapidly point at specific directions (every 15°) rotating only the shoulder (see Fig-
108 ure 1a). The EMGs from nine muscles were recorded during the pointing tasks (see Figure 1b). The
109 EMGs were then processed to extract the phasic part of the movement (Flanders and Herrmann,
110 1992; Flanders et al., 1996; Gaveau et al., 2016; Poirier et al., 2022). To do so, EMG signals were
111 integrated from 1 to 0.5s before movement onset and from 0.5 to 1s after movement stop and
112 averaged. The linear interpolation between those two values was used as an estimate of the tonic
113 component, which was removed from the integrated EMG to keep only the phasic component.
114 Then, all the trials were normalized in duration to 1000 points using linear interpolation.

115 The next step consisted of normalizing EMG amplitude to prepare the input signals for the LDA
116 algorithm. The EMG signals were normalized using a Z-score transformation. It was done sepa-
117 rately for each individual. This reduced the variability which would be caused by inter individual
118 differences in EMG amplitudes. It was also done separately for each muscle, hence ensuring that
119 muscles with small EMG amplitudes were not eliminated from playing a role in classification. Finally,
120 a normalization was done for each angle. This normalization removed information on differences
121 in EMG amplitudes for pointing direction. It was an important step as the differences in amplitude
122 could reflect differences in tonic activity for pointing direction rather than provide information on
123 adjustments in phasic activation.

124 **Linear Discriminant Analysis**

125 Linear discriminant algorithm (LDA) is a classification algorithm which tries to find the best linear
126 hyperplane (hence the name) in the feature space to separate different classes of objects (Grimm

127 **and Yarnold, 2000; Johnson and Wichern, 2007; Izenman, 2008**). This then permits the classification
128 of new observations depending on which side of the hyperplane they are on. Traditionally, LDA
129 was reduced to an eigenvector problem, with the objective of finding a subspace in the original
130 data space that maximize the separability between classes along the first axis of this subspace.
131 However, computational power allows for a more direct approach to classify new data.

132 To achieve this, the algorithm is used to estimate the probability distributions of the different
133 classes, following certain assumptions about these distributions — that both classes follow Gaus-
134 sian distributions with the same variance, but different means. Knowing this information, it is
135 then possible to infer the probability of a new observation to belong to a certain class thanks to
136 Bayes' theorem. This probability is weighted by a cost function to bias the results for particular
137 applications if needed. In practice, the class \hat{y} of a new observation is determined by the following
138 equation:

$$\hat{y} = \arg \min_{y=1, \dots, K} \sum_{k=1}^K \hat{P}(k|x) C(y|k) \quad (1)$$

139 with y and k being class numbers among the K different classes of object.

140 Thus Equation (1) tries to determine, for an observation x , the class k that maximizes $\hat{P}(k|x)C(y|k)$
141 as it is the probability of the observation x to belong to class k . It is determined thanks to the Bayes'
142 theorem :

$$\hat{P}(k|x) = \frac{P(x|k)P(k)}{P(x)} \quad (2)$$

143 $P(k)$ is the prior probability and is determined empirically using the labels distribution from the
144 training set. What the algorithm learn from the data are actually the likelihood distributions $P(x|k)$.
145 In the case of LDA, those distributions are assumed to be multivariate Gaussian distributions, all
146 with the same variance matrices. Thus, the main part of the computation is to find the variance
147 matrix and class means. As the distributions are Gaussian, $P(x|k)$ is entirely determined by the
148 Mahalanobis distance of x for class k . Finally, $P(x)$ is the normalization factor calculated pooling all
149 the estimated $P(x|k)$ distributions :

$$P(x) = \sum_{k=1}^K P(x|k) \quad (3)$$

150 In Equation (1), $C(y|k)$ represent the cost function, *i.e.* how much is penalized the misclassification
151 of an observation. This function can be tweaked for particular usage (*e.g.* to increase sensitivity
152 of the algorithm at the expense of specificity). Here, we do not apply a bias in favor of one class,
153 which then translates to the following cost function :

$$C(y|k) = \begin{cases} 0 & \text{if } y = k \\ 1 & \text{if } y \neq k \end{cases} \quad (4)$$

154 meaning that all classes are equally penalized for misclassification, hence, the hyperplane sep-
155 arating both classes will maximize the separability between the classes and corresponds to the
156 hyperplane that would be obtain through the traditional approach of LDA.

157 Having all the elements needed, \hat{y} can then be determined for any new observation using Equa-
158 tion (1).

159 Additionally, as we did in **Thomas et al. (2023)**, we computed the $LDA_{distance}$ as further indicator
160 of the separation of the data. We defined this value as the Euclidean distance between the means
161 of the Gaussian distributions representing the classes

162 **Support Vector Machine**

163 Like LDA, Support Vector Machines (SVM) are used to find the hyperplane that maximize the sepa-
164 rability between two classes (**Cristianini and Shawe-Taylor, 2000; Hastie et al., 2009**). In our study,
165 we used a linear kernel. However, contrary to LDA which takes into account all the sample of a
166 class, SVM is only interested in the samples from a class that are the closest from the samples of

167 the other class (the so-called support vectors). A margin demarcates each class and the objective
168 of SVM is to maximize the separation between these margins. The optimal separation hyperplane
169 is the one in the middle of the largest margin.

170 This optimal hyperplane can be defined by its orthogonal vector β and a bias vector b so that :

$$f(x) = x^T \beta + b = 0 \quad (5)$$

171 with x being an observation. The objective at this point is to minimize $||\beta||$. However, this approach
172 only works if the two classes are perfectly separable, which may not be the case here, hence we
173 introduce so-called 'slack variables' which will penalize the margin size for each support vector on
174 the wrong side of the separation hyperplane. Thus, the objective becomes to minimize :

$$0.5||\beta||^2 + C \sum \zeta_j \quad (6)$$

175 with respect to β , b and ζ_j subject to $y_i f(x_j) \geq 1 - \zeta_j$ and $\zeta_j \geq 0$ for all $j = 1, \dots, n$. y_j is the label of
176 the observation j (either -1 or 1) and C is a positive scalar called 'box constraint' that regularizes
177 the penalty assigned to errors. To optimize the objective function presented in Equation (6), we
178 use the Lagrange multipliers method. This method introduce a series of coefficients $\alpha_1, \dots, \alpha_n$ which
179 allow the transformation of the objective into maximizing :

$$0.5 \sum_{j=1}^n \sum_{k=1}^n \alpha_j \alpha_k y_j y_k x_j^T x_k - \sum_{j=1}^n \alpha_j \quad (7)$$

180 with respect to $\alpha_1, \dots, \alpha_n$ subject to :

$$\begin{cases} \sum \alpha_j y_j = 0 \\ 0 \leq \alpha_j \leq C \\ \alpha_j [y_i f(x_j) - 1 + \zeta_j] = 0 \\ \zeta_j (C - \alpha_j) = 0 \end{cases} \quad (8)$$

181 for all $j = 1, \dots, n$. Finally, a new observation z is assigned to a class following the equation :

$$\text{sign}(\hat{f}(z)) = \text{sign} \left(\sum_{j=1}^n \hat{\alpha}_j y_j z^T x_j + \hat{b} \right) \quad (9)$$

182 where \hat{b} is the estimate of the bias and $\hat{\alpha}_j$ is the j^{th} estimate of the vector $\hat{\alpha}$. Once classification was
183 done, we used $\frac{2}{||\beta||}$ as an estimate of the size of the margin separating the data.

184 Data Organization for Machine Learning

185 All analyses were performed offline using custom Matlab scripts (**MATLAB, 2022**). The input data
186 was constructed by concatenating the processed EMG signals of the nine muscles. This gave us
187 one vector of 9000 points (1000 normalized time points multiplied by 9 muscles) per trial. Thus, the
188 algorithms were trained on the entire EMG waveforms of all the muscles simultaneously. Further
189 analyses involved focusing on certain parts of the signal. Portions of this vector were isolated as
190 necessary when analyses only involved some muscle subsets (e.g. only the gravity muscles).

191 The training of the algorithms was done using binary classification i.e. the algorithm was trained
192 to discriminate between EMGs of two directions. One of the movement directions was always the
193 horizontal plane (90° , gravity neutral, taken as reference) while the other class was any of the other
194 angles.

195 To ensure the generalization of the results, a stratified five-fold cross-validation method was
196 used. The data set was separated into training and testing sets using the known labels of the
197 samples to ensure that both directions were equally represented in each training and testing set.
198 The cross-validation approach allowed a better estimation of the efficacy of the algorithm by testing

199 it on multiple data sets. Thus, we were able to compute an average accuracy of the algorithm on
200 several testing sets.

201 From each trained LDA algorithm, we extracted the means of the two $P(x|k)$ distributions as
202 well as the testing accuracy. Then, we computed the $LDA_{distance}$ measuring the separation between
203 the mean vectors of each class. For SVM algorithms, we extracted the vector orthogonal to the
204 separation hyperplane and computed the width of the margin.

205 **Statistical analysis**

206 The significance of results was obtained using non-parametric tests, namely the Wilcoxon rank
207 sum test when comparing two conditions and the Friedman test to compare effects across multiple
208 conditions. Results were considered to be significant for $p < 0.05$.

209 **Results**

210 The processed phasic EMGs from the recorded nine muscles for every pointing angle can be seen
211 in Figure 2. We will start the result section with a presentation of a grid displaying the classification
212 accuracies of individual muscles versus the accuracy obtained from all the muscles. The main pur-
213 pose of this would be to illustrate the higher accuracies obtained from using the combined muscle
214 information. We will then continue examining the classification obtained using all the muscles si-
215 multaneously in order to trace the nature of collective muscular tuning for pointing direction. The
216 nature of this tuning will be further analyzed using the $LDA_{distance}$. From using input vectors which
217 contain the information from all the muscles, we will then turn to analyzing specific groups of mus-
218 cles. Once again, classification accuracies will be used as an indicator of adaptation for pointing
219 direction, hence allowing us to trace tuning curves for particular muscle groups. Finally, as one
220 of the major points of this paper is that the negative portions of the phasic EMGs are a result of
221 gravity effort optimization, we will use classification to see if this portion of the EMG is tuned to
222 pointing direction. Results obtained using LDA will also be reinforced using the SVM as an alternate
223 Machine Learning algorithm.

224 **Advantage of a multimuscle approach**

225 The aim of this section is to demonstrate some of the benefits of a multimuscle approach. In
226 Figure 3 we display a grid with the classification accuracies of individual muscles for each pointing
227 angle as well as the accuracy using all the muscles simultaneously (last line of grid). For almost
228 all directions, the classification accuracy using all the muscles is higher than those obtained with
229 individual muscles. This demonstrates that information concerning differences in muscular activity
230 for pointing in different directions may be found at the level of the muscle population even when
231 it may not be significantly present at the level of individual muscles.

232 Other features of note in this figure are that some muscles like the anterior deltoid, have rel-
233 atively high accuracies when pointing at 0° as well as at 180° , hence indicating an important role
234 in adaptation for both directions. This is not the case for a muscle like the medial deltoid which
235 displays high accuracies for pointing at 180° , but not for 0° . The short triceps has low accuracies
236 in discriminating for any angle, hence showing that it does not have a prominent role in adapting
237 for direction.

238 **Binary classification with all muscles for pointing direction**

239 The aim of this section is to follow the nature of multimuscle adaptation for pointing in each of the
240 seventeen directions described in the Methods section. Using all the muscles, LDA was used to
241 detect if pointing had taken place horizontally or at another pointing direction. Figure 4 displays
242 the accuracies from this classification of 90° (horizontal pointing) versus another angle displayed
243 on the x-axis. Poor classification accuracies reflect small separation between data groups while a
244 good accuracy is indicative of clear separation. The EMG tuning curves using this technique display
245 adjustments which are mostly linear until approximately 60° from horizontal direction. Following

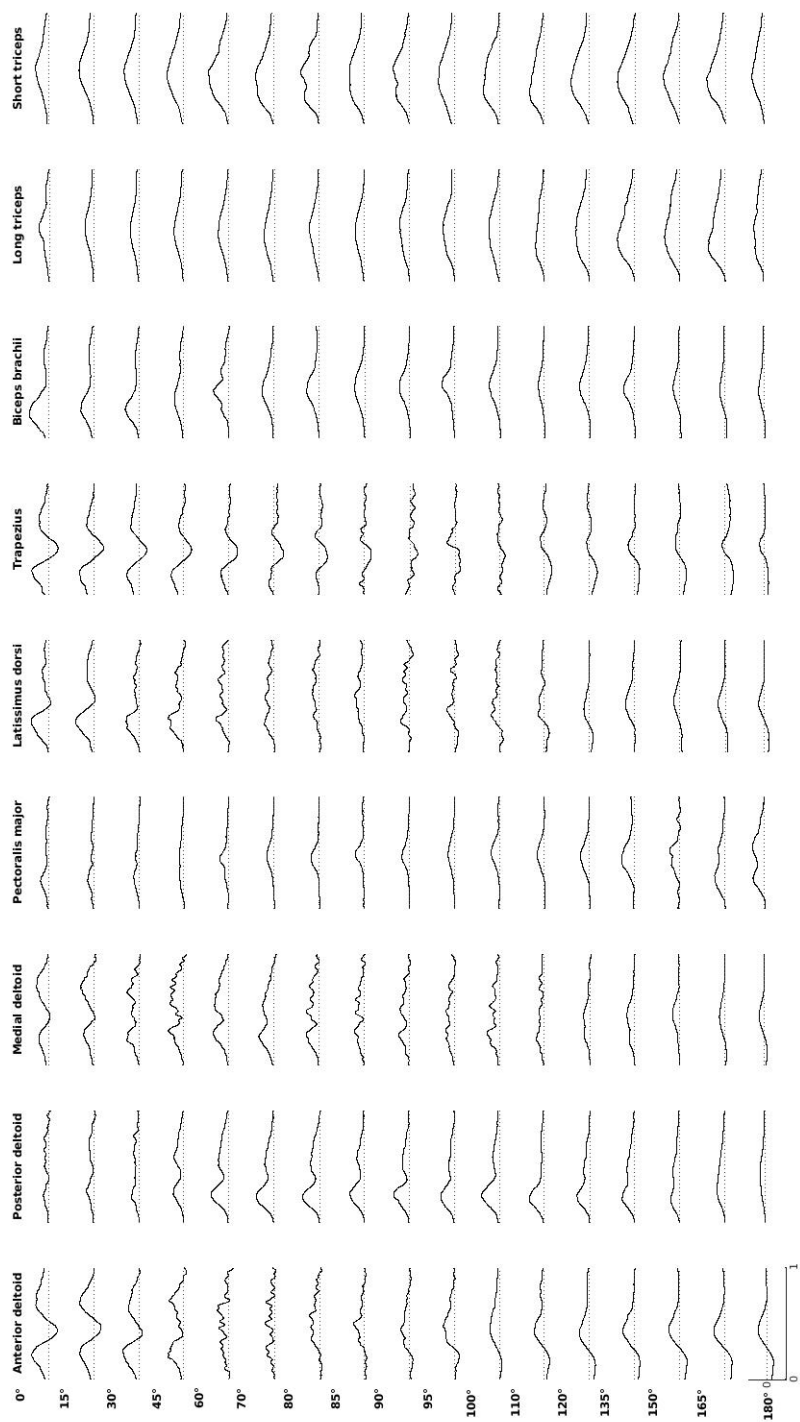


Figure 2. Example of EMG recordings (averaged among all trials from one participant). Data was normalized by the highest recorded phasic activity of the participant.

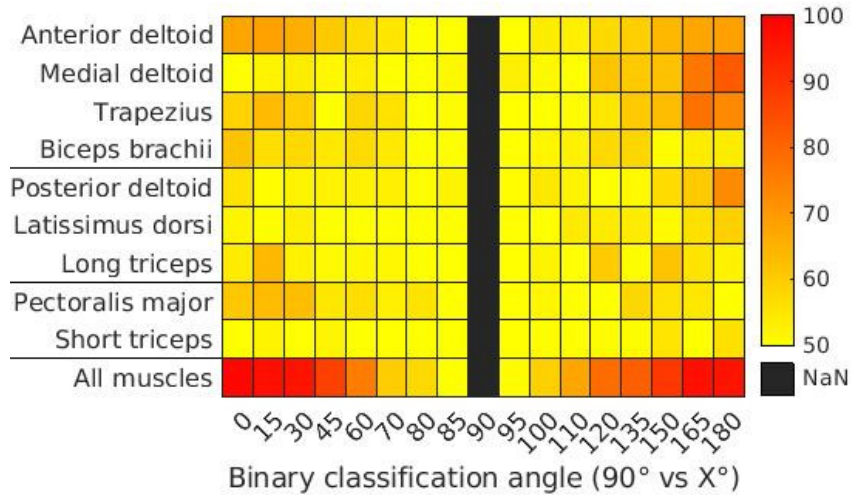


Figure 3. Average binary accuracy of individual and all muscles for different angles compared to 90°, using LDA for classification. The muscles are ordered by their type (anti-gravity, gravity and neutral) and lines separate the different types of muscles.

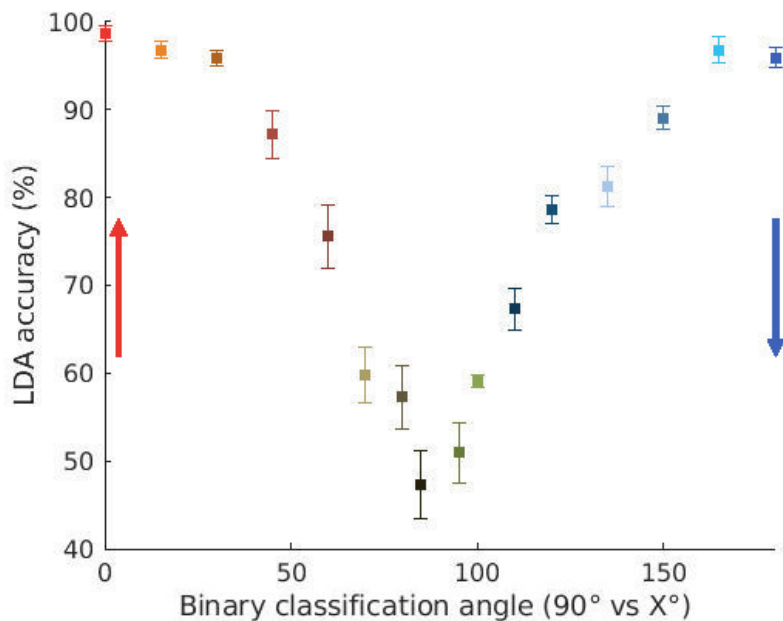


Figure 4. Accuracy of the binary classification between 90° and the other angles, using the EMGs from all muscles for LDA classification. Error bars indicate standard error. Arrows indicate pointing directions considering as origin the horizontal axis (90°). The colors indicate pointing directions as in Figure 1a.

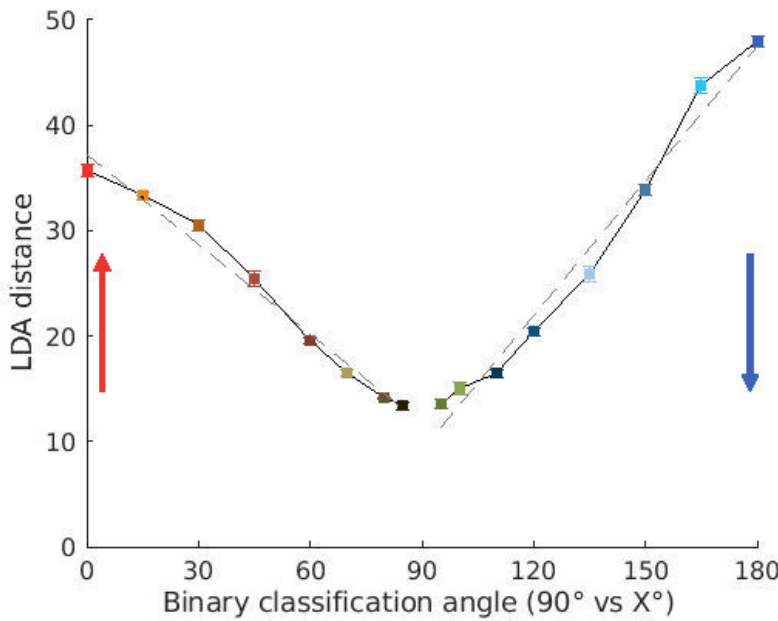


Figure 5. $LDA_{distance}$ computed from the models of each category constructed by the classification algorithm for binary discrimination between 90° and the other angles using all muscles (see Methods). Error bars indicate standard error. Gray dashed lines show the linear regressions performed for comparing upward versus downward tuning. The colors indicate pointing directions as in Figure 1a.

246 this, classification accuracies took a non-linear trend. Similar trends were observed when performing
247 the same classification with the SVM (Supplementary Figure S1).

248 The non-linearity in binary classification may not be due to actual non-linear muscular modifi-
249 cation but due to saturation in classification capacities (see Supplementary Figure S9). Verification
250 as to whether this was the case, was done by further examining the model used by LDA to perform
251 the classification.

252 The multivariate mean of each category is an important piece of information used by LDA to
253 create representations of each category. The distance between these means can be exploited
254 to measure muscular tuning for pointing direction. Figure 5 displays how this distance changes
255 as a function of pointing direction. The figure confirms a linear trend in collective muscular tun-
256 ing for pointing direction until about 60° from horizontal. However, unlike classification accuracy,
257 $LDA_{distance}$ is not subject to the effects of classification saturation. Muscular modification as re-
258 flected in the $LDA_{distance}$ s continue increasing with a slightly nonlinear trend both upwards to 0°
259 and downwards to 180° .

260 The $LDA_{distance}$ also revealed an intriguing aspect of muscular tuning for pointing direction. It
261 showed that adjustments for downward pointing are bigger than those for upward pointing when
262 compared to pointing in the horizontal direction. The $LDA_{distance}$ for pointing at 0° upward was
263 found to be significantly lower than the distance for pointing at 180° downward (Wilcoxon rank
264 sum $W = 0$, $p = 0.008$). Differences in the gain for tuning were also revealed by fitting a regres-
265 sion line for both sides of the EMG tuning curves. They revealed a value of 0.2839 ($R^2 = 0.9852$)
266 for upward pointing and 0.4257 ($R^2 = 0.9795$) for downward movements indicating once again that
267 counter to intuition, movements were more finely tuned in the downward direction. Further confi-
268 rmation of this difference in upward and downward adaptation can be seen in the Supplementary
269 Figure S2 where we measure the distance from both groups using another classification algorithm,
270 the Support Vector Machine (SVM, Wilcoxon rank sum $W = 0$, $p = 0.008$).

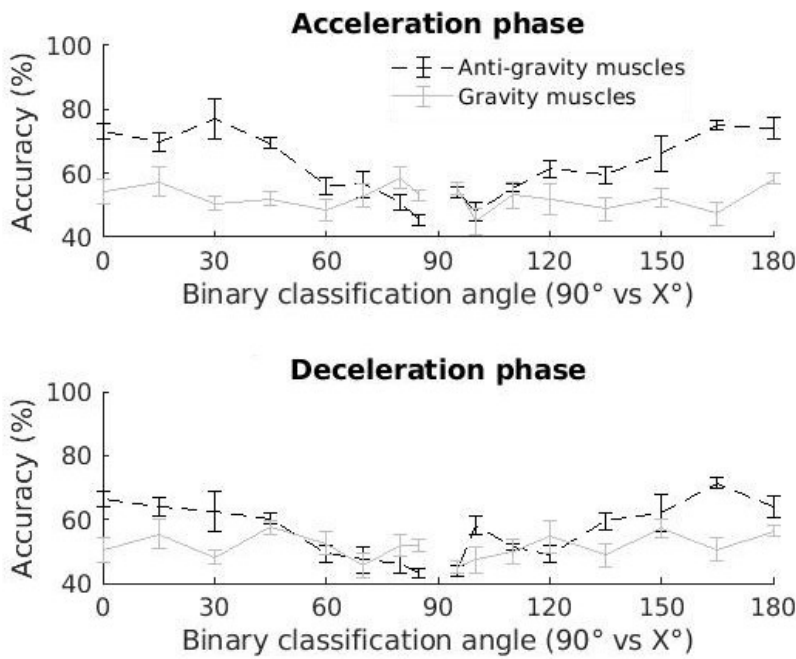


Figure 6. Classification accuracy using only the EMGs from either gravity or antigravity muscles during the acceleration or deceleration phase of the movement, using LDA for classification.

271 Modular EMG tuning for pointing direction

272 As the system adapts for tuning in various directions, what is the nature of this tuning? Does
273 the entire system undergo modifications to bring the arm to a new direction i.e. a uniform tuning?
274 Or is adaptation for pointing to the new direction primarily accomplished by a few muscles at
275 particular moments, i.e. modular tuning? To answer this question, we examined the classification
276 capacities of different groups of muscle at different moments. The muscle groups were the gravity
277 and antigravity muscles. A finer grained analysis of modularity was obtained by examining the
278 acceleration and deceleration halves for the aforementioned muscle groups. The gravity muscles
279 in this study are the posterior deltoid, the latissimus dorsi and long triceps. The antigravity muscles
280 are the anterior deltoid, medial deltoid, trapezius and biceps brachii. Figure 6 below demonstrates
281 the classification accuracy of these muscle groupings. Taking the case of the acceleration phase it
282 can be seen that the antigravity muscles achieved a significantly superior performance at predicting
283 pointing direction when compared to the gravity muscles (Friedman test, $\chi^2(1) = 26.35$, $p < 0.001$).

284 As there were 4 antigravity muscles but only 3 gravity muscles, it was necessary to verify that
285 the higher classification accuracies observed in the antigravity muscles was not due to more infor-
286 mation. To do this, we repeated the classification tests after having removed the biceps brachii
287 from the group of antigravity muscles (this muscle showed the poorest tuning among the group
288 of antigravity muscles, see Figure 3). The prediction capacities of the antigravity muscles remain
289 significantly higher than those of the gravity muscles (Friedman test, $\chi^2(1) = 10.39$, $p = 0.001$, see
290 Supplementary Figure S4).

291 Table 1a shows the values for the slopes of these lines for each group of muscles for upward and
292 downward pointing in Figure 6. They reveal higher slopes for the antigravity muscles at all phases
293 of upward and downward pointing. Of note, are the slopes of the antigravity muscles during the
294 acceleration phase of downward movement and the deceleration phase of upward movement.
295 As these are phases during which the antigravity muscles have lowered activity, it indicates that
296 the deactivation in these muscles is not an all-or-nothing function, but one that is graduated as a
297 function of pointing direction. The lower values of the slopes for the gravity muscles demonstrate
298 relatively smaller adjustments by this group of muscles for pointing angles.

(a) Acceleration phase

	Upward movements	Downward movements
Antigravity muscles	0.3306 ($R^2 = 0.80$)	0.2910 ($R^2 = 0.90$)
Gravity muscles	0.0041 ($R^2 = 0.001$)	0.0315 ($R^2 = 0.051$)

(b) Deceleration phase

	Upward movements	Downward movements
Antigravity muscles	0.2895 ($R^2 = 0.93$)	0.233 ($R^2 = 0.67$)
Gravity muscles	0.0183 ($R^2 = 0.02$)	0.0983 ($R^2 = 0.49$)

Table 1. Slope coefficients of the linear regressions for the classification accuracy of the different muscle groups from Figure 6.

299 All these results were further confirmed using another classification algorithm, the SVM. These
300 results can be seen in Supplementary Figure S5.

301 Tuning with the negative portions of the antigravity muscles

302 An important tenet of the gravity effort-optimization hypothesis is that the muscles are able to re-
303 duce their activity in conditions where gravity is able to replace their role. In the case of EMG phasic
304 activity, this would especially be seen during the negative phases of this activity, primarily at the
305 latter half of upward movement (deceleration) and the first half of downward movement (accel-
306 eration). Figure 6 which examines tuning in the group of antigravity muscles for the acceleration and
307 deceleration halves of pointing already hints at the likelihood of tuning in this phase. Neverthe-
308 less, the acceleration and deceleration phases of the antigravity muscles still contain portions of
309 the EMG which are positive. In this section we zone in further to examine the tuning capacities of
310 the portions of the phasic EMGs for the antigravity muscles which are exclusively negative. Figure 7
311 contains the results of these tests. Once again, the increasing classification accuracy of this por-
312 tion of the phasic EMG as a function of pointing direction, indicates adjustments as a function of
313 pointing direction. Further confirmation of tuning in this negative portion of the EMG was obtained
314 using the SVM classification algorithm (Supplementary Figure S7).

315 Discussion

316 In this study we examined the manner in which phasic activity of shoulder muscles are adjusted for
317 arm pointing movements in different directions. This extends previous results demonstrating that
318 arm kinematics is tuned to pointing direction (**Gaveau et al., 2016**). The researchers had demon-
319 strated that effort optimization leads to clear differences in phasic muscular activity for vertically
320 upward and downward pointing. The authors had also showed qualitatively that this integration
321 can be seen at the muscular level (**Gaveau et al., 2021**). The current study extends on these two
322 previous studies by providing a much finer grained, quantitative picture of phasic muscular tuning
323 for pointing direction. More specifically, through the use of relatively recent quantitative tools, it
324 analyzes the information content in the negative portions of the phasic EMG.

325 A key finding of the study is that the negative portion of the phasic EMGs contains information
326 concerning pointing direction. Many previous studies had set aside this part of the EMG as unim-
327 portant and the inevitable result of the computation required to extract phasic activity (**d'Avella
328 et al., 2008; Russo et al., 2014**). The presence of information in this section of the EMG is especially
329 clear from Figure 7 (and Supplementary Figure S7) where Machine Learning was used to automati-
330 cally detect if the unlabeled negative portions of the EMGs of antigravity muscles could be used to
331 predict whether a subject had performed horizontal pointing or pointing at some other specified
332 angle. The figure shows that in many cases, accuracy was above chance levels. It also shows that
333 the classification accuracy changed as a function of pointing direction. As explained in the Intro-

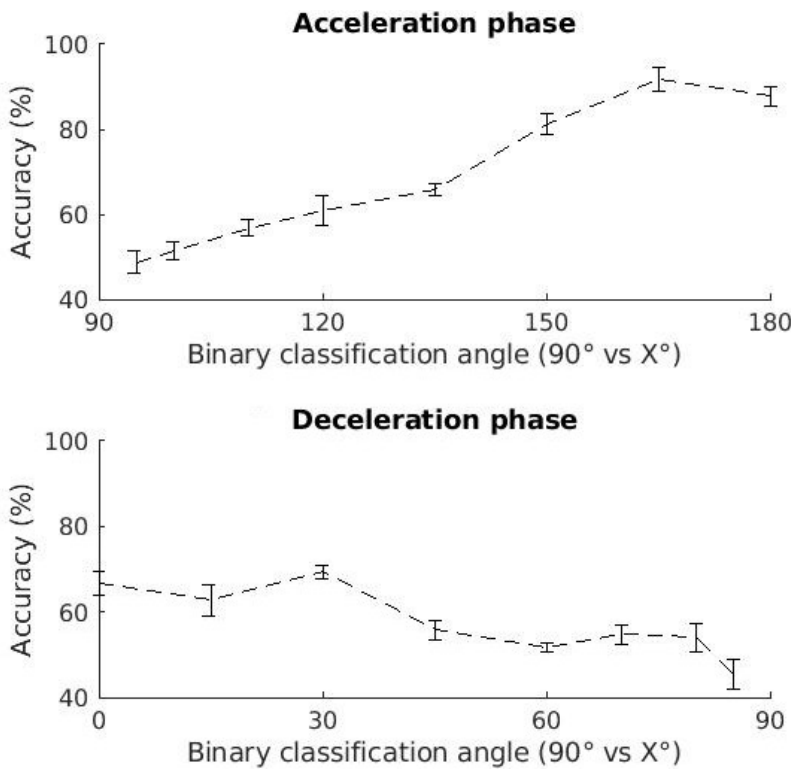


Figure 7. Classification accuracy using only the negative part of the EMGs from antigravity muscles during the acceleration or deceleration phase of the movement, using LDA for classification.

duction section, classification accuracy is an indicator of data separability. The increasing classification accuracy with increasing angular separation from horizontal indicates that the deactivation in these negative phases were not on-off functions but scaled in accordance with pointing angle. An on-off deactivation function that does not change with pointing angle would have given similar classification accuracies (perhaps above chance) for all pointing angles. A better idea of the information content in the negative portions of the phasic EMGs can also be obtained by examining the classification accuracies obtained using the positive portions of the phasic EMGs (Supplementary Figure S8). It can be see here that the tuning curves do not attain classification accuracies that are higher than those of the negative portions.

Another original aspect of the study is the use of Machine Learning in order to obtain an ensemble view of muscle activation patterns. Tuning of muscles for different pointing directions was analysed in terms of classification accuracy. The prediction of task constraints using Machine Learning algorithm was done with combined muscular activity as input. This approach is interesting in view of the synergistic manner in which muscles achieve task goals. The term synergistic refers to the fact that movement is the result of the combined activities of several muscles in which the role of any one muscle in the group need not remain constant as others can compensate for this inconsistency and still achieve the original goal. The term Motor Equivalence also refers to this idea (Lashley, 1933; Morasso, 2022). An ensemble analysis therefore has the potential to provide insight into group properties which may not be present at the single muscle level or worse yet, at the level of a single EMG parameter such as amplitude or onset delay. A single variable of this sort may not have sufficient power to reach statistical significance. This is clearly demonstrated in Figure 3 where the last line displays the classification accuracy obtained from the combination of all the muscles recorded during the experiments. It is darker than any of the preceding lines hence indicating a higher discrimination power for the muscle population.

The main machine learning technique used for the study was LDA. This technique was primarily

359 chosen because of its simplicity and ease of understanding the features which are critical to the
360 classification (*Thomas et al., 2023*). As a technique which is not as powerful as methods which were
361 developed later (*Statnikov et al., 2008; Nair et al., 2010; Heung et al., 2016; Han et al., 2018; Uddin
362 et al., 2019*), there was also a lower risk of classification saturation (see Supplementary Figure S9).
363 By this we mean high classification accuracies from very small differences, leading to poor infor-
364 mation concerning differences in data separability for different pointing angles. We address this
365 problem in Figure 5 where LDA_{distance} was used to probe data separation in situations where clas-
366 sification accuracy had reached a plateau of close to 100%. Our fears on this question turned out
367 to be unfounded when we used the SVM with a linear kernel for the supplementary figures of the
368 current study (Supplementary Figures S1, S2, S5, S6, S7). True to its reputation as a more powerful
369 classifier, the SVM did indeed provide generally higher accuracies but displayed tuning curves with
370 patterns similar to those obtained using the LDA algorithm, hence backing up the results obtained
371 with LDA.

372 Figure 5 (and Supplementary Figure S2) presents the intriguing result that the EMG separation
373 is higher in the downward direction than upward. One possible explanation of this may be that
374 both upward and horizontal pointing follow the classical triphasic burst pattern (*Hallett et al., 1975;
375 Virji-Babul et al., 1994*). In contrast to this, Gaveau et al had predicted (2016) and demonstrated
376 (2021) a very different pattern of muscular activity for downward pointing. In accordance with the
377 effort optimisation hypothesis they showed that the antigravity muscles phasic activity becomes
378 negative during the first half of downward pointing, hence leading to an activity pattern which is
379 quite different from what is seen for horizontal pointing.

380 A similar explanation could be used to explain the differences in the tuning curves of Figure 6
381 (and Supplementary Figure S5). The tuning curves of these figures and Table 1 display a sharper
382 tuning for pointing direction in the antigravity muscles than for the gravity muscles (higher slopes
383 in accuracy as a function of pointing direction). This difference in tuning may be due to the fact
384 that the negative portions of the phasic EMGs are not present in the gravity muscles. The poorer
385 tuning of the gravity muscles may be due to this absence and hence underscores the important
386 role played by the negative portions of the phasic EMGs in adjusting for pointing direction.

387 Figure 3 displays the accuracies of each muscle for pointing in different directions individually.
388 The accuracy patterns of the anterior deltoid show that it is tuned in both directions. The trapezi-
389 ius shows a similar pattern of classification accuracies, though their smaller values would indicate
390 smaller adjustments than the anterior deltoid. In contrast to the two aforementioned muscles, the
391 phasic activity of the medial and posterior deltoids are more tuned for downward pointing, show-
392 ing higher accuracies for distinguishing downward than upward pointing angles. The importance
393 of all these muscles in pointing have been highlighted by various studies (*Flanders, 1991; Flanders
394 et al., 1994, 1996; Mira et al., 2021; Tokuda et al., 2016*). In contrast to the previous studies, the
395 use of classification accuracy allows for a greater ease in comparing and contrasting the roles of
396 individual muscles. A direct comparison with the previous studies is not possible, as the pointing
397 protocols were often different, involving for example, mobility around the elbow joint. In contrast
398 to the previously mentioned muscles, the short triceps displays poor classification accuracies at
399 all angles in both directions. Once again, this does not necessarily mean that the muscle is not
400 active, but that it is poorly distinguishable from its activity for horizontal pointing, and hence does
401 not play an important role in tuning for direction. This is not unexpected as this mono-articular
402 muscle is involved in keeping the elbow joint extended but not in rotating the shoulder joint.

403 No discussion on ensemble methods would be complete without talking about matrix factor-
404 ization methods. These techniques have been very useful in demonstrating that the panoply of
405 EMG recordings from the arm during pointing under different constraints can be simplified by us-
406 ing a small number of basis functions which can then be adapted for multiple constraints (*d'Avella
407 et al., 2008; Muceli et al., 2010; d'Avella and Lacquaniti, 2013*). The technique which was frequently
408 applied was non negative matrix factorization (NNMF). Therein lies the problem for analyzing a por-
409 tion of the phasic EMG which this study has found to be important – the negative portion. Since

410 it is a technique with non-negativity constraints, NNMF is not adapted to the study of the nega-
411 tive portions of the phasic EMG. This problem has recently been addressed with the mixed matrix
412 factorization method (MMF) (*Scano et al., 2022, 2023*). Even though, like Machine Learning, these
413 matrix factorization methods are ensemble methods taking into account global properties of big
414 collections of data, they have a very different focus when compared to Machine Learning classifica-
415 tion. Their emphasis is on finding commonalities between the collection of EMG trajectories while
416 Machine Learning classification centers on finding differences. The two methods are therefore
417 complementary to each other. It should be noted that in many fields, the two methods are some-
418 times used sequentially. Matrix factorization is often used in the feature extraction step to first
419 reduce spatial dimensionality before then going on to apply Machine Learning (*Duda, 2000*). This
420 step was not taken in our study as it would have complicated the process of trying to understand
421 the features which were critical to classification.

422 In conclusion, we will say that Machine Learning classification shows that the antigravity mus-
423 cles are better tuned to pointing direction than the gravity muscles. Focusing on the deactivation
424 portions of these phasic EMGs, our study demonstrates that they are modified for pointing direc-
425 tion. Previous studies by *Gaveau et al. (2021)* supported the hypothesis that this negativity would
426 result from integrating gravity for optimized motor control. They had not however, studied the
427 nature of this muscular adjustment in fine detail. Using the EMG patterns from nine muscles and
428 pointing in 17 directions, the current study shows that the deactivation of the antigravity muscles
429 is not an on-off function, but is adjusted as a function of pointing direction.

430 References

431 **Arrieta AB, Díaz-Rodríguez N, del Ser J, Bennetot A, Tabik S, Barbado A, García S, Gil-López S, Molina D, Ben-**
432 **jamins R, Chatila R, Herrera F. Explainable Artificial Intelligence (XAI): Concepts, Taxonomies, Opportunities**
433 **and Challenges toward Responsible AI. Information Fusion. 2020 Jun; 58. <https://hal.archives-ouvertes.fr/hal-02381211>, doi: 10.1016/j.inffus.2019.12.012, publisher: Elsevier.**

435 **Atkeson CG, Hollerbach JM. Kinematic features of unrestrained vertical arm movements. Journal of Neuro-**
436 **science. 1985 Sep; 5(9):2318–2330. <https://www.jneurosci.org/content/5/9/2318>, doi: 10.1523/JNEUROSCI.05-**
437 **09-02318.1985**, publisher: Society for Neuroscience Section: Articles.

438 **Bernshtain NA. The Co-ordination and Regulation of Movements. Pergamon Press; 1967. Google-Books-ID:**
439 **F9dqAAAAMAAJ.**

440 **Brambilla C, Scano A. The Number and Structure of Muscle Synergies Depend on the Number of Recorded**
441 **Muscles: A Pilot Simulation Study with OpenSim. Sensors (Basel, Switzerland). 2022 Nov; 22(22):8584. doi:**
442 **10.3390/s22228584.**

443 **Burdet E, Osu R, Franklin DW, Milner TE, Kawato M. The central nervous system stabilizes unstable dynamics**
444 **by learning optimal impedance. Nature. 2001 Nov; 414(6862):446–449. doi: 10.1038/35106566.**

445 **Cristianini N, Shawe-Taylor J. An Introduction to Support Vector Machines and Other Kernel-**
446 **based Learning Methods. Cambridge: Cambridge University Press; 2000. <https://www.cambridge.org/core/books/an-introduction-to-support-vector-machines-and-other-kernelbased-learning-methods/A6A6F4084056A4B23F88648DDBFDD6FC>, doi: 10.1017/CBO9780511801389.**

449 **d'Avella A, Fernandez L, Portone A, Lacquaniti F. Modulation of phasic and tonic muscle synergies with reaching**
450 **direction and speed. Journal of Neurophysiology. 2008 Sep; 100(3):1433–1454. doi: 10.1152/jn.01377.2007.**

451 **d'Avella A, Lacquaniti F. Control of reaching movements by muscle synergy combinations. Frontiers in Com-**
452 **putational Neuroscience. 2013 Apr; 7:42. <https://www.ncbi.nlm.nih.gov/pmc/articles/PMC3630368/>, doi:**
453 **10.3389/fncom.2013.00042.**

454 **Duda RO. Pattern Classification 2e. 2nd édition ed. New York: Wiley–Blackwell; 2000.**

455 **Farshchian A, Sciutti A, Pressman A, Nisky I, Mussa-Ivaldi FA. Energy exchanges at contact events guide sensori-**
456 **motor integration. eLife. 2018 May; 7:e32587. <https://doi.org/10.7554/eLife.32587>, doi: 10.7554/eLife.32587**,
457 **publisher: eLife Sciences Publications, Ltd.**

458 **Flanders M. Temporal patterns of muscle activation for arm movements in three-dimensional space. The**
459 **Journal of Neuroscience: The Official Journal of the Society for Neuroscience. 1991 Sep; 11(9):2680–2693.**

460 **Flanders M, Herrmann U. Two components of muscle activation: scaling with the speed of arm movement.**
461 **Journal of Neurophysiology. 1992 Apr; 67(4):931–943. doi: 10.1152/jn.1992.67.4.931.**

462 **Flanders M, Pellegrini JJ, Soechting JF. Spatial/temporal characteristics of a motor pattern for reaching. Journal**
463 **of Neurophysiology. 1994 Feb; 71(2):811–813. <https://journals.physiology.org/doi/abs/10.1152/jn.1994.71.2.811>, doi: 10.1152/jn.1994.71.2.811**,
464 **publisher: American Physiological Society.**

465 **Flanders M, Pellegrini JJ, Geisler SD. Basic features of phasic activation for reaching in vertical**
466 **planes. Experimental Brain Research. 1996 Jun; 110(1):67–79. <https://doi.org/10.1007/BF00241376>, doi:**
467 **10.1007/BF00241376.**

468 **Franklin DW, Wolpert DM. Computational mechanisms of sensorimotor control. Neuron. 2011 Nov; 72(3):425–**
469 **442. doi: 10.1016/j.neuron.2011.10.006.**

470 **Gaveau J, Berret B, Angelaki DE, Papaxanthis C. Direction-dependent arm kinematics reveal optimal integration**
471 **of gravity cues. eLife. 2016 Nov; 5:e16394. <https://doi.org/10.7554/eLife.16394>, doi: 10.7554/eLife.16394**,
472 **publisher: eLife Sciences Publications, Ltd.**

473 **Gaveau J, Grospretre S, Berret B, Angelaki DE, Papaxanthis C. A cross-species neural integration of gravity for**
474 **motor optimization. Science Advances. 2021 Apr; 7(15):eabf7800. <https://www.ncbi.nlm.nih.gov/pmc/articles/PMC8026131/>, doi: 10.1126/sciadv.abf7800.**

476 **Grimm LG, Yarnold PR, editors. Reading and Understanding More Multivariate Statistics. 1st edition ed. Wash-**
477 **ington, DC: Amer Psychological Assn; 2000.**

478 **Hagen DA**, Valero-Cuevas FJ. Similar movements are associated with drastically different muscle contraction
479 velocities. *Journal of Biomechanics*. 2017 Jul; 59:90–100. doi: [10.1016/j.jbiomech.2017.05.019](https://doi.org/10.1016/j.jbiomech.2017.05.019).

480 **Hallett M**, Shahani BT, Young RR. EMG analysis of stereotyped voluntary movements in man. *Journal of*
481 *Neurology, Neurosurgery, and Psychiatry*. 1975 Dec; 38(12):1154–1162. <https://www.ncbi.nlm.nih.gov/pmc/articles/PMC492181/>.

483 **Han T**, Jiang D, Zhao Q, Wang L, Yin K. Comparison of random forest, artificial neural networks and sup-
484 port vector machine for intelligent diagnosis of rotating machinery. *Transactions of the Institute of*
485 *Measurement and Control*. 2018 May; 40(8):2681–2693. <https://doi.org/10.1177/0142331217708242>, doi:
486 10.1177/0142331217708242, publisher: SAGE Publications Ltd STM.

487 **Hastie T**, Tibshirani R, Friedman J. *The Elements Of Statistical Learning: Data Mining, Inference, And Prediction*,
488 Second Edition. 5e édition ed. New York, NY: Springer-Verlag New York Inc.; 2009.

489 **Heung B**, Ho HC, Zhang J, Knudby A, Bulmer CE, Schmidt MG. overview and comparison of machine-learning
490 techniques for classification purposes in digital soil mapping. *Geoderma*. 2016; <https://doi.org/10.1016/j.geoderma.2015.11.014>, publisher: Elsevier B.V.

492 **Hollerbach JM**, Flash T. Dynamic interactions between limb segments during planar arm movement. *Biological*
493 *Cybernetics*. 1982 May; 44(1):67–77. <https://doi.org/10.1007/BF00353957>, doi: 10.1007/BF00353957.

494 **Izenman AJ**. *Modern Multivariate Statistical Techniques: Regression, Classification, and Manifold Learning*. 1st
495 ed. 2008, corr. 2nd printing 2013 edition ed. New York ; London: Springer; 2008.

496 **Johnson RA**, Wichern DW. *Applied Multivariate Statistical Analysis*. 6th edition ed. Upper Saddle River, NJ:
497 Pearson; 2007.

498 **Laroche D**, Tolamby A, Morisset C, Maillefert JF, French RM, Ornetti P, Thomas E. A classification study of
499 kinematic gait trajectories in hip osteoarthritis. *Computers in Biology and Medicine*. 2014 Dec; 55:42–48.
500 doi: [10.1016/j.combiomed.2014.09.012](https://doi.org/10.1016/j.combiomed.2014.09.012).

501 **Lashley KS**. Integrative functions of the cerebral cortex. *Physiological Reviews*. 1933 Jan; 13(1):1–42. <https://journals.physiology.org/doi/abs/10.1152/physrev.1933.13.1.1>, doi: [10.1152/physrev.1933.13.1.1](https://doi.org/10.1152/physrev.1933.13.1.1), publisher: American Physiological Society.

504 **Latash ML**. The Bliss of Motor Abundance. *Experimental brain research Experimentelle Hirnforschung Experi-
505 mentation cerebrale*. 2012 Mar; 217(1):1–5. <https://www.ncbi.nlm.nih.gov/pmc/articles/PMC3532046/>, doi:
506 10.1007/s00221-012-3000-4.

507 **MATLAB**. MATLAB version: 9.13.0 (R2022b). Natick, Massachusetts, United States: The MathWorks Inc.; 2022.
508 <https://www.mathworks.com>.

509 **Mira RM**, Molinari Tosatti L, Sacco M, Scano A. Detailed characterization of physiological EMG activations and
510 directional tuning of upper-limb and trunk muscles in point-to-point reaching movements. *Current Research*
511 *in Physiology*. 2021 Jan; 4:60–72. <https://www.sciencedirect.com/science/article/pii/S2665944121000092>, doi:
512 [10.1016/j.crphys.2021.02.005](https://doi.org/10.1016/j.crphys.2021.02.005).

513 **Morasso P**. A Vexing Question in Motor Control: The Degrees of Freedom Problem. *Frontiers in Bioengineering*
514 *and Biotechnology*. 2022; 9. <https://www.frontiersin.org/articles/10.3389/fbioe.2021.783501>.

515 **Muceli S**, Boye AT, d'Avella A, Farina D. Identifying representative synergy matrices for describing muscular
516 activation patterns during multidirectional reaching in the horizontal plane. *Journal of Neurophysiology*.
517 2010 Mar; 103(3):1532–1542. doi: [10.1152/jn.00559.2009](https://doi.org/10.1152/jn.00559.2009).

518 **Murdoch WJ**, Singh C, Kumbier K, Abbasi-Asl R, Yu B. Definitions, methods, and applications in inter-
519 pretative machine learning. *Proceedings of the National Academy of Sciences of the United States of*
520 *America*. 2019 Oct; 116(44):22071–22080. <https://www.ncbi.nlm.nih.gov/pmc/articles/PMC6825274/>, doi:
521 [10.1073/pnas.1900654116](https://doi.org/10.1073/pnas.1900654116).

522 **Nair SS**, French RM, Laroche D, Thomas E. Application of Least-squares kernel methods and Neural Network
523 Algorithms to the classification of Electromyographic patterns in Arthritis patients. *IEEE Transactions on*
524 *Neural Systems and Rehabilitation Engineering*. 2010; 18(2):174–184.

525 **Poirier G**, Papaxanthis C, Lebigre M, Juranville A, Mathieu R, Savoye-Laurens T, Manckoundia P, Mourey
526 F, Gaveau J. Aging decreases the lateralization of gravity-related effort minimization during vertical
527 arm movements. *bioRxiv*; 2023. <https://www.biorxiv.org/content/10.1101/2021.10.26.465988v3>, doi:
528 [10.1101/2021.10.26.465988](https://doi.org/10.1101/2021.10.26.465988), pages: 2021.10.26.465988 Section: New Results.

529 **Poirier G**, Papaxanthis C, Mourey F, Lebigre M, Gaveau J. Muscle effort is best minimized by the right-dominant
530 arm in the gravity field. *Journal of Neurophysiology*. 2022 Apr; 127(4):1117-1126. <https://journals.physiology.org/doi/full/10.1152/jn.00324.2021>, doi: [10.1152/jn.00324.2021](https://doi.org/10.1152/jn.00324.2021), publisher: American Physiological Society.

532 **Russo M**, D'Andola M, Portone A, Lacquaniti F, d'Avella A. Dimensionality of joint torques and muscle patterns
533 for reaching. *Frontiers in Computational Neuroscience*. 2014; 8. <https://www.frontiersin.org/articles/10.3389/fncom.2014.00024>.

535 **Scano A**, Brambilla C, Russo M, d'Avella A, Upper limb phasic muscle synergies with negative weight-
536 ings: applications for rehabilitation. *TechRxiv*; 2023. https://www.techrxiv.org/articles/preprint/Upper_limb_phasic_muscle_synergies_with_negative_weightings_applications_for_rehabilitation/22795553/1, doi:
538 [10.36227/techrxiv.22795553.v1](https://doi.org/10.36227/techrxiv.22795553.v1).

539 **Scano A**, Mira RM, d'Avella A. Mixed matrix factorization: a novel algorithm for the extraction of kinematic-
540 muscular synergies. *Journal of Neurophysiology*. 2022 Feb; 127(2):529-547. <https://journals.physiology.org/doi/full/10.1152/jn.00379.2021>, doi: [10.1152/jn.00379.2021](https://doi.org/10.1152/jn.00379.2021), publisher: American Physiological Society.

542 **Statnikov A**, Wang L, Aliferis CF. A comprehensive comparison of random forests and support vector machines
543 for microarray-based cancer classification. *BMC bioinformatics*. 2008 Jul; 9:319. doi: [10.1186/1471-2105-9-319](https://doi.org/10.1186/1471-2105-9-319).

545 **Thomas E**, Ali FB, Tolamby A, Chambellant F, Gaveau J. Too much information is no information: how machine
546 learning and feature selection could help in understanding the motor control of pointing. *Frontiers in Big
547 Data*. 2023; 6. <https://www.frontiersin.org/articles/10.3389/fdata.2023.921355>.

548 **Tokuda K**, Lee B, Shiihara Y, Takahashi K, Wada N, Shirakura K, Watanabe H. Muscle activation patterns in
549 acceleration-based phases during reach-to-grasp movement. *Journal of Physical Therapy Science*. 2016 Nov;
550 28(11):3105-3111. doi: [10.1589/jpts.28.3105](https://doi.org/10.1589/jpts.28.3105).

551 **Tolamby A**, Chiovetto E, Pozzo T, Thomas E. Modulation of anticipatory postural activity for mul-
552 tiple conditions of a whole-body pointing task. *Neuroscience*. 2012 May; 210:179-190. doi:
553 [10.1016/j.neuroscience.2012.02.050](https://doi.org/10.1016/j.neuroscience.2012.02.050).

554 **Tolamby A**, Thomas E, Chiovetto E, Berret B, Pozzo T. An Ensemble Analysis of Electromyographic Activity
555 during Whole Body Pointing with the Use of Support Vector Machines. *PLoS ONE*. 2011 Jul; 6(7):e20732.
556 <https://www.ncbi.nlm.nih.gov/pmc/articles/PMC3144191/>, doi: [10.1371/journal.pone.0020732](https://doi.org/10.1371/journal.pone.0020732).

557 **Uddin S**, Khan A, Hossain ME, Moni MA. Comparing different supervised machine learning algorithms for
558 disease prediction. *BMC medical informatics and decision making*. 2019 Dec; 19(1):281. doi: [10.1186/s12911-019-1004-8](https://doi.org/10.1186/s12911-019-1004-8).

560 **Virji-Babul N**, Cooke JD, Brown SH. Effects of gravitational forces on single joint arm movements in hu-
561 mans. *Experimental Brain Research*. 1994 May; 99(2):338-346. <https://doi.org/10.1007/BF00239600>, doi:
562 [10.1007/BF00239600](https://doi.org/10.1007/BF00239600).

563 **Supplementary Material**

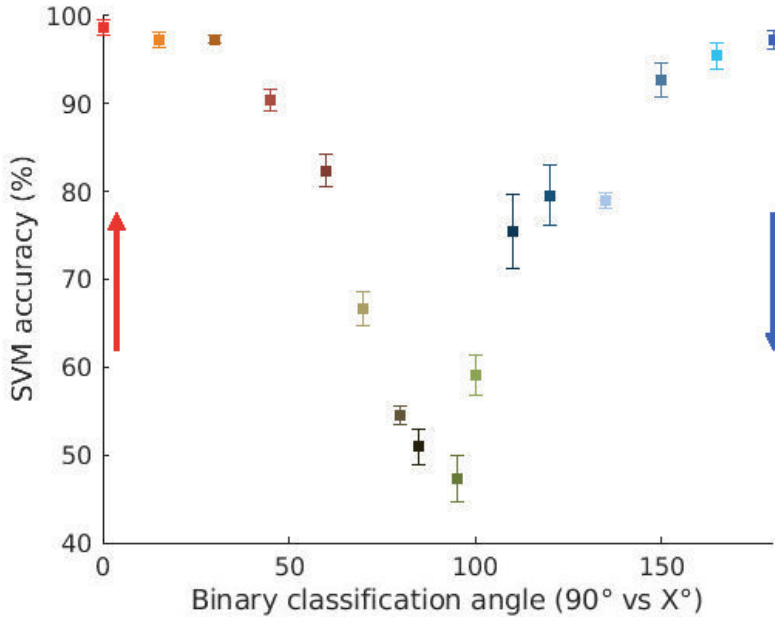


Figure S1. Accuracy of the binary classification when using EMGs from all the muscles. Classification was done for pointing between between 90° and the other angles, using SVM for classification. Error bars indicate standard error. The colors indicate pointing directions as in Figure 1a.

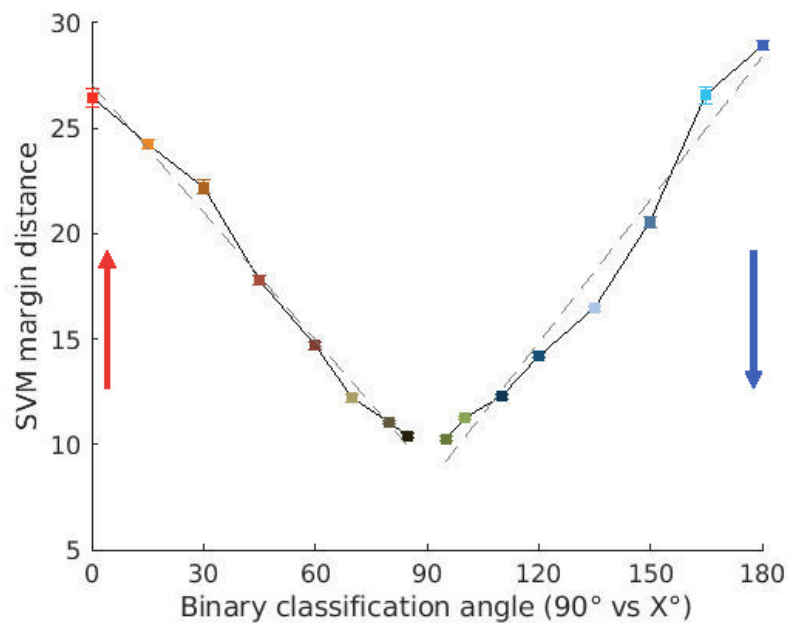


Figure S2. Size of the estimated SVM margin using EMGs from all muscles. Error bars indicate standard error. The colors indicate pointing directions as in Figure 1a.

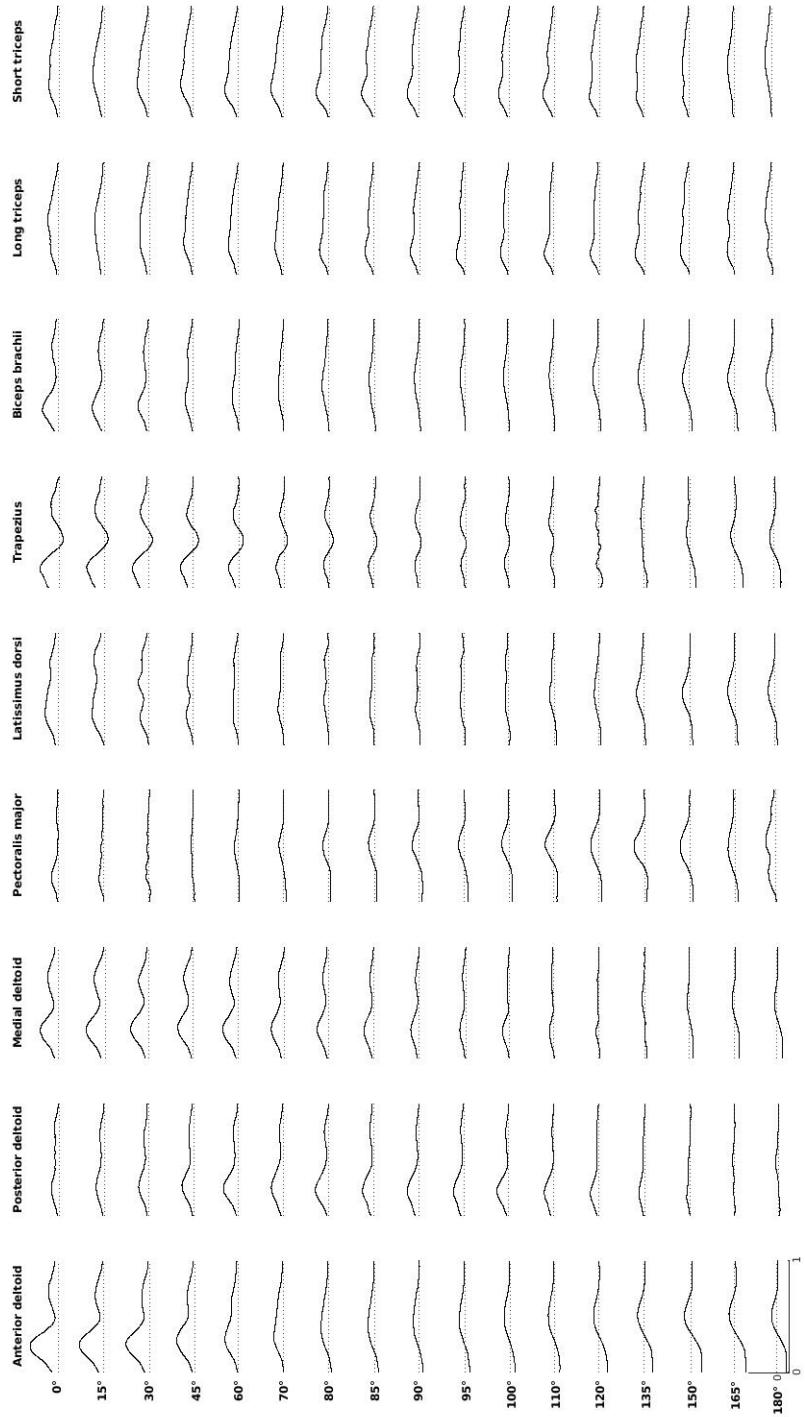


Figure S3. Average of the EMG recordings from all participants. Data was normalized by the highest recorded phasic activity of each participant.

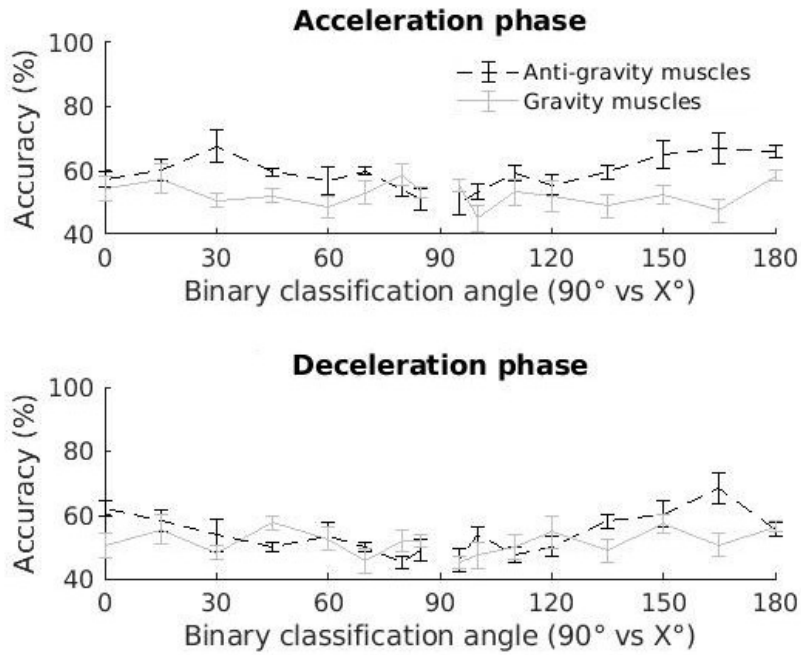


Figure S4. Classification accuracy using only the EMGs from either gravity or antigravity muscles. Contrary to Figure 6, the biceps brachii is not included in the antigravity muscles here, using LDA for classification.

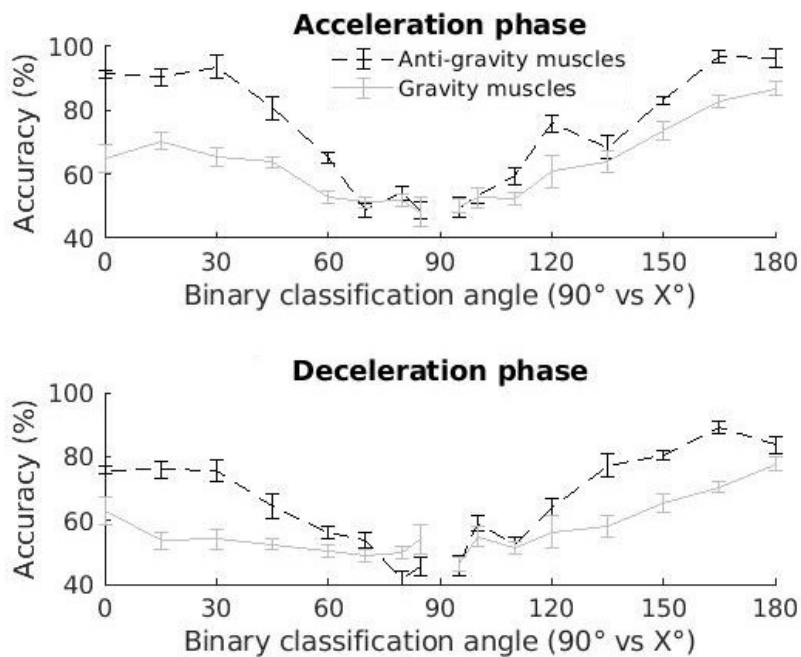


Figure S5. Classification accuracy using only the EMGs from either gravity or antigravity muscles during the acceleration phase of the movement or the deceleration phase, using SVM for classification.

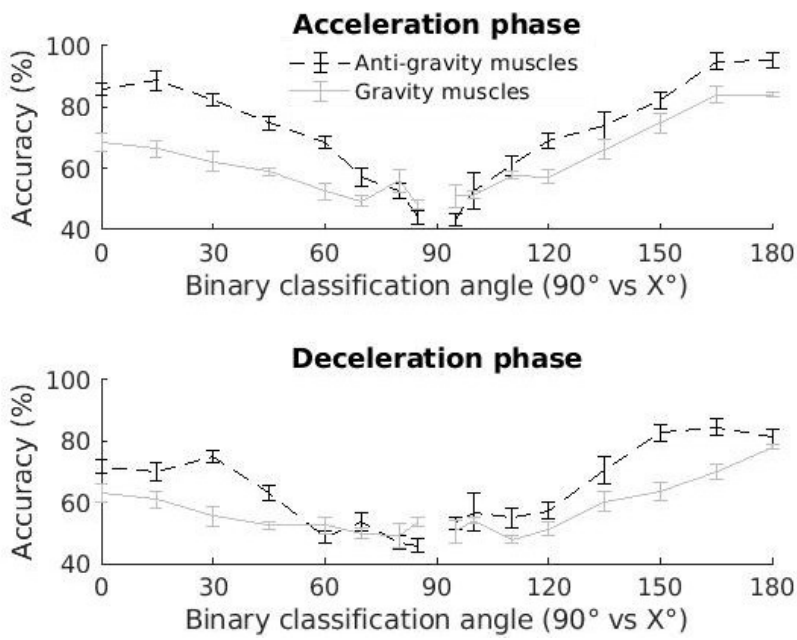


Figure S6. Classification accuracy using only the EMGs from either gravity or antigravity muscles during the acceleration phase of the movement or the deceleration phase, using SVM for classification. Contrary to Figure S5, the biceps brachii is not included in the antigravity muscles here.

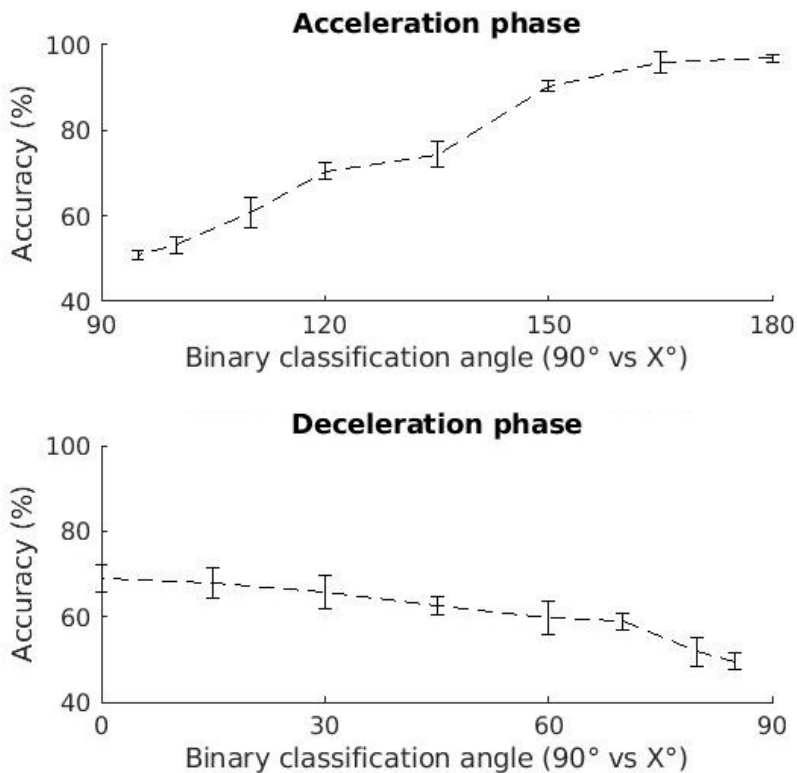


Figure S7. Classification accuracy using only the negative part of the EMGs from antigravity muscles during the acceleration phase of the movement or the deceleration phase, using SVM for classification.

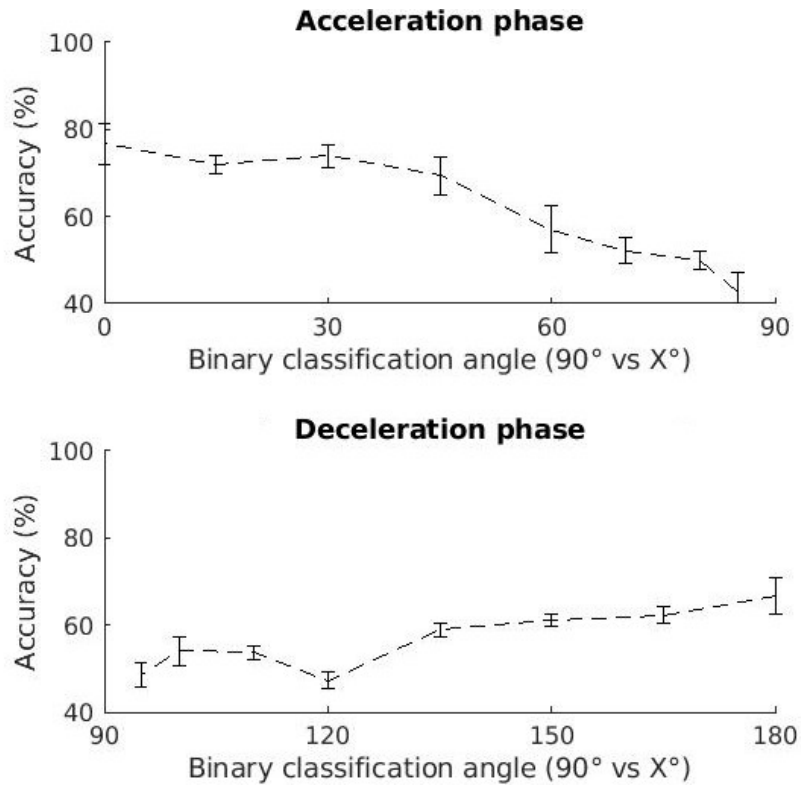


Figure S8. Classification accuracy using only the positive part of the EMGs from antigravity muscles, using LDA for classification.

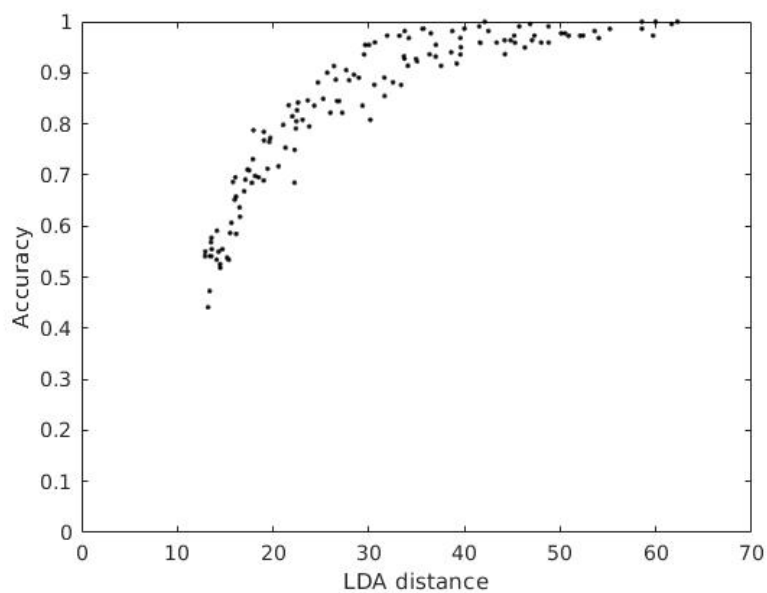


Figure S9. Accuracy as a function of the LDA_{distance}.